J. COMBIN. MATH. COMBIN. COMPUT. 127a (2025) 363--379

Journal of Combinatorial Mathematics and Combinatorial Computing
www.combinatorialpress.com/jcmcc

Combinatorial Press

Research on physical properties of shale gas reservoirs in Hunan Province based on the analysis model of logging data

Yan Li[1], Wenshi Wang[1,✉], Jie Wang[1], Xu Dong[1], Lihong He[2]

[1] *Changsha General Survey of Natural Resources Center, China Geological Survey, Ningxiang, Hunan, 410600, China*

[2] *Geophysical and Geochemical Survey Institute of Hunan Province, Hunan Green Intelligent Exploration Engineering Technology Research Center, Changsha, Hunan, 410014, China*

ABSTRACT

Most areas in Hunan Province are rich in shale gas blocks, and their shale gas reservoir physical properties, geological characteristics, and enrichment rules need to be further studied. The article chooses the five # logging data of the Xiaoyanxi Formation in Anhua, Hunan Province, as the research object, preprocesses the logging data by curve environmental influence correction, curve reconstruction, and normalization, calculates the total organic carbon content and mineral composition change of shale gas by multiple linear regression, and uses the multi-mineral content calculated by optimization algorithm combined with the volumetric model to realize the matrix porosity of the variable skeleton. Then, the differential equivalent medium, self-compatible approximation, and K-T models were used to calculate the shale rock skeleton modulus. Then the shale gas reservoir petrophysical model was constructed. The adsorbed gas and free gas of the shale gas reservoir were solved separately to obtain the total gas content of the shale gas reservoir. The average TOC content solved by the model is 1.79%, which is only 2.23% higher than the absolute error of the actual data. When the volume fraction of the organic matter mixture increased from 0 to 0.25, the relative change of the longitudinal and transverse wave velocity ratio was only 0.87%. The shale gas content in Anhua Xiaoyanxi Formation 5# in Hunan Province ranges from 0.87 to 8.41 cm^3/g, significantly higher than the lower limit value for shale gas industrial development. Recorded well data can clarify the reservoir's physical characteristics of shale gas in Hunan Province and provide data support for exploring shale gas.

Keywords: curve reconstruction; total organic carbon content; K-T model; gas content; shale gas; logging data

✉ Corresponding author.

E-mail address: wwsvictory@126.com (W. Wang).

Received 05 April 2024; Revised 18 September 2024; Accepted 16 November 2024; Published Online 15 April 2025.

DOI: 10.61091/jcmcc127a-022

1. Introduction

At present, the world energy is coinciding into the development era of oil, natural gas, coal, nuclear energy and renewable energy, and traditional fossil energy is still the main primary energy consumption [1-4]. According to the International Energy Agency forecast in May 2012, by 2035, the proportion of natural gas in the world's primary energy consumption structure reached 25%, becoming the second largest primary energy source after oil [5-6]. Between 2010 and 2035, global demand for natural gas will rise by more than 50%, equal to the growth of coal, oil and nuclear energy combined. And shale gas-dominated unconventional natural gas production will amount to two-thirds of the increased natural gas supply during the period [7-8]. It can be seen that the exploration, development and utilization of shale gas is heating up rapidly worldwide, and shale gas, as a representative of unconventional natural gas, has a great development advantage [9-10].

With the deepening degree of exploration of conventional oil and gas resources, unconventional oil and gas resources such as shale gas reservoirs have become an important source of oil and gas scale increase in storage and production [11-12]. Shale reservoirs are characterized by low porosity, poor permeability, diverse mineral components, rich in organic matter, non-uniform distribution of fluids, significant anisotropy, non-homogeneity, and complex pore structure, which leads to uncertainties in seismic petrophysics (elastic properties of rocks, medium propagation velocity, density, and other parameters), and increases the multiplicity of solutions for the fine description of shale reservoirs [13-16]. Therefore, considering the complex microphysical characteristics of shale reservoirs, the establishment of a reasonable and effective rock physics model for anisotropic shale reservoirs can provide theoretical guidance for clarifying the petrophysical response mechanism of shale and predicting the physical property parameters [17-18].

In recent years, although the measurement technology of rock physical property parameters has been continuously improved, factors affecting the measurement results and data accuracy have emerged, including rock sample processing methods, testing conditions, and calculation models [19-20]. Therefore, it is extremely important to establish relevant experimental conditions, improve the accuracy and consistency of experimental data, and determine the most suitable physical property parameter measurement methods for Chinese shales [21].

To solve the contradiction between the shortage of oil and gas resources and the sharp increase in demand, the exploration scope of shale gas is continuously expanded, and clarifying the physical changes of shale gas storage helps to better explore the layout of shale gas. In this paper, five # of Anhua Xiaoyanxi Formation in Hunan Province is selected as the research object, its geological conditions are analyzed, and curve reconstruction, normalization, and other preprocessing operations are carried out on its logging data to ensure the consistency and reliability of the data. Multiple linear regression model was used to construct the calculation model of TOC, the K curve was used to calculate the rock mineral content, and the volume model combining multiple mineral contents was established through the optimization algorithm to solve the mixed skeleton value of shale to obtain the matrix porosity of shale. The Backus average theory was introduced to construct the anisotropic rock matrix associated with the laminated structure. The anisotropic Krief theory was applied to establish the rock skeleton. The Brown-Korringa theory was used to add fluids into the dry porosity to construct the petrophysical model of the saturated shale. Based on the linear relationship between the Langmuir volume and the total organic carbon content, the shale's adsorbed gas content and free gas content were also solved to obtain the total gas content of the shale gas. The logging data analyzed the physical parameters, petrophysical changes, and gas content of the shale gas reservoirs in-depth, providing accurate data support for expanding the exploration scope of shale gas in Hunan Province.

2. Logging data preprocessing and shale gas reservoir physical properties

Hunan Province is located in the combination of Yangzi and Huaxia land masses and has experienced six major tectonic evolution stages and five tectonic gyres, with excellent metallogenic geological conditions, good endowment conditions, rich mineral resources, obvious resource advantages, and great potential for mineral search. According to the strategic mineral domestic mineral search action and Hunan's strategic needs, combined with the characteristics of mineral resources endowment in Hunan Province, we can deeply analyze the changes of shale gas reservoir physical parameters in Hunan Province. It can strengthen the basic geological work, clarify the shale gas storage layout, and contribute to Hunan Geological Exploration to support national energy resources' security and serve the beautiful blueprint of "three highs and four news."

2.1 Pre-processing of logged well data in the study area

2.1.1 Geological conditions of the study area. The geotectonic position of the shale gas investigation area of Hunan Anhua Cambrian Xiaoyanxi Formation is in the section where the arc tectonics of Jiangnan-Xuefeng Rise changes from north-north-east to north-east-north-east, and the main part belongs to the Xuefeng Mountain basement fold-impact fault zone. Folds and ruptures are very developed in the area, and there are many faults parallel to the folds in the northeast-north-east tectonic belt, which are mostly oblique thrust reverse faults in nature. The study area is located on the southeastern edge of the Xuefengshan uplift. The southern part of the area is separated from the Xiangzhong depression by the Anhua-Xupu rupture. The tectonic main body of the area is dominated by the Northeast-Northeast oriented Sawmuling compound syncline, which extends up to 40km transversely, with the core part of the Silurian system and the Ordovician and Aurignacian systems exposed on the wings of the ends in turn. The Cambrian system is widely distributed on the surface of the area; the middle and lower part of the area is the clastic rock, mainly composed of mud shale; the upper part is composed of carbonate rock and clastic rock, the carbonate rock accounts for more, the thickness of the stratum is more than 600 m. The Ordovician system is well developed, the lithology is relatively stable, and it is mainly composed of clastic and carbonate rock. The thickness of the stratum is about 1,000 m. The Zhiliu system is not well developed; obviously, most of the area is stripped, and the thickness dominates the lithology of about 1900m.

With the ablation of regional glaciers in the late Early Aurignacian, the tension between the Yangzi and Huaxia plates intensified. The sea level in the early Late Aurignacian of the study area rose significantly, and sea erosion occurred. In the late Late Aurignacian, the water body deepened in the area south of the fracture due to the influence of the Dayong-Cili syn-sedimentary fracture zone. In the Early Cambrian, due to the continuous tensile fracture and trapping, the sea level in the area rose rapidly, which was the period of the greatest sea erosion, forming a deep water body with a deeper shelf-basin phase environment and the deposition of the Xiaoyanxi Formation formed a thick layer of dark organic-rich shale, which is a favorable target layer for shale gas exploration in the area.

2.1.2 Logging Data Preprocessing. In this paper, the logging data from the shale gas investigation area of Anhua, Hunan Province, is used as the research data source. Quality control is necessary for the original logging data to ensure consistency and reliability. The pre-processing of logging data is the basis for ensuring the accuracy of logging interpretation and evaluation. In this paper, based on the original logging data, we mainly carry out the work of environmental impact correction, curve reconstruction, and normalization of logging curves.

1) Correction of environmental influence of logging curve. In the actual logging environment, factors such as the density and mineralization of mud, temperature, and pressure of the formation, as well as the expansion of mudstone in contact with water, borehole collapse, etc., often cause the logging curves to be distorted, which cannot fully reflect the real information of the formation. As the data basis for lithology

identification and reservoir parameter calculation, the logging curve determines the precision and accuracy of shale gas reservoir logging evaluation and interpretation. In view of this, to reduce the environmental impact of the logging curve, it is necessary to correct the logging curve.

In view of the subsequent lithology identification, parameter modeling and other work need density data, so this paper carries out the density curve correction, the correction model is:

$$L_c = L + \frac{a\left(D_{cal} - D_{bits}\right)}{D_{bits}} + b \tag{1}$$

Where L, L_c is the recording value to be corrected and corrected respectively, D_{cal} is the recording diameter value, D_{bits} is the bit diameter value, and a and b are the correction coefficients.

2) Recording curve reconstruction. In view of the lack of acoustic time difference curve in some wells in the study area, this paper carries out the reconstruction of acoustic time difference logging curve through Gardner formula. The proposed empirical formula for sonic velocity and density is:

$$\rho = \mathrm{k}v^m \tag{2}$$

where ρ is the density, v is the acoustic velocity, and $\mu\mathrm{s/m, k, m}$ is the scale factor. Thereafter, an empirical relationship between acoustic velocity and resistivity was proposed as:

$$v = A \times R_t^{\ B} \tag{3}$$

where A, B is the fitting coefficient and R_t is the resistivity.

3) Recorded well curve normalization processing. In shale reservoir parameter modeling, it is necessary to use the normalized logging data as the input, therefore, this paper carries out the normalization of logging information to prepare the data for the subsequent algorithm modeling. In this paper, the normalization process is carried out for each recorded well curve, and the calculation formula is:

$$N = (X_T - X_{\min}) / (X_{\max} - X_{\min}) \tag{4}$$

2.2 *Shale gas reservoir evaluation parameters*

2.2.1 Total Organic Carbon Content and Mineral Composition:

1) Total organic carbon content. The total organic carbon content of shale gas reservoir physical properties is affected by multiple factors (formation lithology, depositional environment, pore fluid and organic matter), so the quantitative prediction of the total organic carbon content by single-element fitting method is poorly evaluated [22]. In this paper, based on the relationship between total organic carbon content and logging curves, we selected appropriate logging curves and established a multiple regression analysis model to improve the calculation accuracy of the total organic carbon content model of shale formations.

The correlation between the total organic carbon content and the density curve and the U curve in the gamma energy spectroscopy logging is good, and the multiple regression mathematical model of the total organic carbon content and the density curve (DEN) and the U curve established. Namely:

$$TOC = a \times U + b \times \rho + c \tag{5}$$

TOC is total organic carbon content, U is uranium curve recording readings, ρ is density recording curve readings, and a, b, c is curve fit values.

2) Mineral composition calculation. The mineral composition of Hunan Anhua shale is complex, and at present the conventional logging data are mainly used to evaluate the rock mineral content. It is usually considered that the natural gamma (GR), potassium content (K), thorium content (TH) and uranium-free

gamma (KTH) have a better relationship with the clay content, so the K curve is chosen to calculate the rock mineral content.

The clay mineral calculation model is as follows, which is realized in two main steps:

First, the clay content index $CLAY$ was calculated using the change in the relative value of potassium (DK), viz:

$$CLAY = DK = \frac{K - K_{\min}}{K_{\max} - K_{\min}} \tag{6}$$

where K is the recorded potassium value, $K_{\max}$ is the potassium value of the mudstone layer, $K_{\min}$ is the potassium value of the sandstone, and DK is the relative potassium value.

The clay content index $CLAY$ is then converted to clay content V_{CLAY}, i.e:

$$V_{CLAY} = \frac{2^{GCUR \times CALY} - 1}{2^{GCUR} - 1} \tag{7}$$

where V_{GLAY} is the clay content and $GCUR$ is the stratigraphic constant.

2.2.2 Shale Gas Reservoir Physical Property Evaluation Parameters. Based on the geological profile of Anhua shale gas in Hunan Province, it is difficult to evaluate the reservoir space in detail by conventional methods. For matrix hole calculation, due to the complexity of lithology, the correlation between experimental analysis and logging values is poor. For this reason, we use the multi-mineral content calculated by the optimization algorithm combined with the volume model to find the value of the mixed skeleton, and realize the matrix porosity of the variable skeleton ϕ. Then:

$$\rho_{ma} = \rho_{qu} \times v_{qu} + \rho_{cl} \times v_{cl} + \rho_{ca} \times v_{ca} + \rho_{do} \times v_{do} + \rho_{K-f_e} \times v_{K-fe} \tag{8}$$

$$\phi = \frac{\rho_b - \rho_{ma}}{\rho_f - \rho_{ma}} \tag{9}$$

where ρ_{ma} is the hybrid skeleton value.

For the qualitative and quantitative description of cracks, the most accurate and intuitive method is to use high-definition images of electro-imaging to evaluate, which can get the type, size, and production of cracks, etc. The quantitative evaluation is mainly to quantify the openness (width), density, length, and porosity of cracks picked up [23]. Currently, the more widely used application is to quantify the crack width using the finite element method, with the formula:

$$W = cA\rho_m^b \rho_{xo}^{1-b} \tag{10}$$

where W is the fracture width, c and b are constants, instrument-dependent, depending on the specific structure of the imaging logging instrument, A is the area of anomalous current caused by the fracture, ρ_m is the mud filtrate resistivity, which is generally measured by conventional logging, and ρ_{xo} is the flushing zone resistivity, which is generally taken directly from the value of the electro-imaging micro-resistivity that has been graduated through the shallow lateral direction.

3. Petrophysical modeling and gas content evaluation of shale reservoirs

Shale gas means that the main body is located in dark mud shale or high carbon mud shale, and the generation, storage, and capping all occur in the shale system, which is a typical "in situ" reservoir model. In shale gas logging evaluation, reservoir physical parameters such as total organic carbon content, porosity, and mineral composition are very important. In addition, the physical properties of shale gas reservoirs and shale gas content have a certain influence, and exploring the changes in shale gas content can help better shale gas exploitation and ensure the energy supply of shale gas.

3.1 *Petrophysical modeling of shale gas reservoirs*

3.1.1 Petrophysical modeling process. The significance of anisotropy is that while the direction changes, the physical, chemical, and other properties of the material change along with it, with each direction exhibiting different properties. The anisotropic characteristics of geologic bodies lead to different propagation velocities in different directions in shale gas exploration. Therefore, anisotropic petrophysical modeling studies play an important role in the characterization of gas-bearing properties of shale gas reservoirs.

Figure 1 shows the schematic diagram of the petrophysical modeling. According to the macroscopic anisotropic characteristics of the target reservoir, the anisotropic rock matrix associated with the laminar structure is constructed through the Backus average theory, and the mineral matrix includes minerals such as clay, calcite, dolomite, and quartz. To introduce randomly distributed inorganic dry pores into the mineral matrix, the anisotropic Krief theory must be applied to build the rock skeleton [24]. Since the inorganic dry pores contain fluids, the Brown-Korringa theory can be applied to add fluids to the dry pores to build a saturated shale matrix.

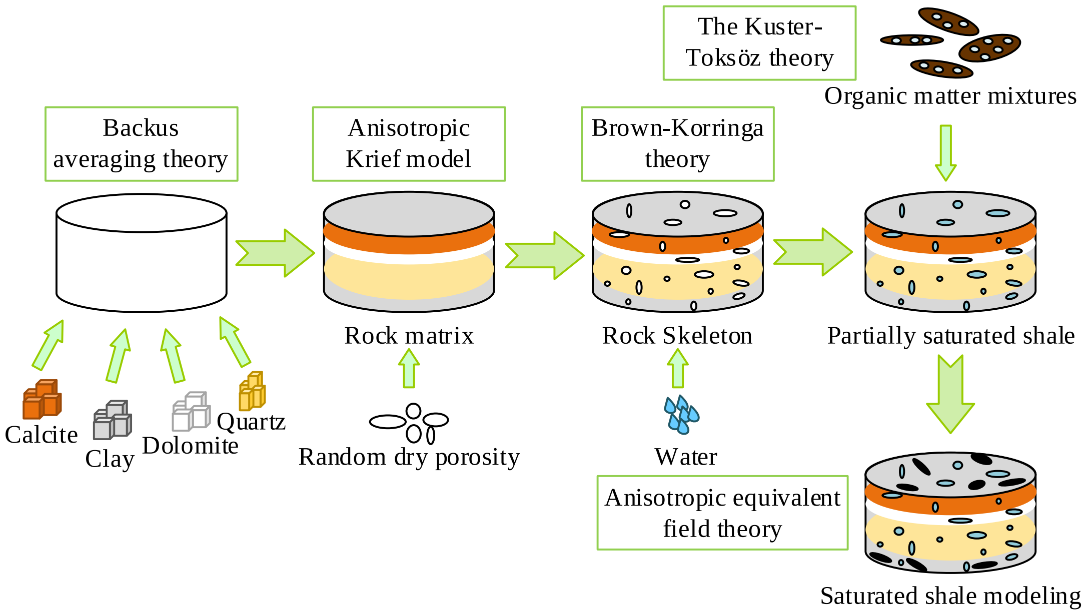

Fig. 1. Modeling process of rock physical model

In addition, there is an organic matter mixture in shale gas reservoirs, which consists of organic matter and organic pores and fluids; therefore, in the petrophysical modeling process, organic pores and fluids can be fused with organic matter (casein) to form the organic matter mixture through the Kuster-Toksȍz theory. To merge the organic matter mixture and saturated shale matrix to model the shale gas reservoir, the anisotropic equivalent field theory needs to be applied to introduce the organic matter mixture into the saturated shale matrix, and ultimately, the saturated shale model is constructed.

3.1.2 Shale gas petrophysical modeling. Rock Physical Modeling (RPM) is an important tool for connecting elastic parameters, rock, and pore fluid properties, and the sources of elastic anisotropy in shale include the intrinsic properties of clay minerals, dominant alignment directions of clay minerals, casein grains, non-spherical pores, and microfractures. For this reason, the petrophysical modeling process in this paper is divided into four main steps as follows:
1) Average the mixed minerals to obtain the matrix.
2) Add pores and fluids to the matrix.
3) Add microfractures and fluids.
4) Add inclined fractures and fluids.

In the first step, the elastic parameters of the shale mineral matrix were calculated using VRH averaging and H-S averaging, respectively.H-S averaging takes into account the order of the mineral compositions, and calculations when hard minerals are defined as the first material are set as the upper bound [25]. The upper and lower bounds calculated using these two methods are:

$$M_{voigt} = \sum_{i=1}^{N} f_i M_i \tag{11}$$

$$M_{Reuss} = \sum_{i=1}^{N} \frac{f_i}{M_i} \tag{12}$$

$$K^{HS\pm} = K_1 + \frac{f_2}{\left(K_2 - K_1\right)^{-1} + f_1\left(K_1 + \frac{4}{3}\mu_1\right)^{-1}} \tag{13}$$

$$\mu^{HS\pm} = \mu_1 + \frac{f_2}{\left(\mu_2 - \mu_1\right)^{-1} + \frac{2 f_1\left(K_1 + 2\mu_1\right)}{5\mu_1 K_1 + \frac{4}{3}\mu_1}} \tag{14}$$

where M, K and μ are the modulus of elasticity and f is the volume fraction of minerals.

In the second and third steps, the Differential Equivalent Medium (DEM) model, the Self-Compatible Approximation (SCA) model, and the K-T model are used to calculate the skeleton modulus, respectively. Moreover, the theoretical assumptions of the KT model are limited to sparsely arranged inclusion, which is no longer applicable to the case of large porosity.The DEM model is compatible with both low and high porosity, can be applied to both shale and siltstone, and can be further extended to anisotropy. Therefore, the rock skeleton of shale was calculated using the DEM model.

Based on the fracture development characteristics of the shale, an inclined fracture model was used in the fourth step to consider the oblique angle of the fracture, aspect ratio and fracture density for the calculation. The equivalent stiffness coefficient of the fracture-containing rock is:

$$C_{etf} = (M + H)^{-1} \tag{15}$$

where M and H are the flexibility coefficient matrices of the background medium and the crack, respectively, and H can be written as:

$$H = \begin{bmatrix} 0 & 0 & 0 & 0 & 0 & 0 \\ 0 & Z_T \sin^2\theta & 0 & -Z_T \sin\theta\cos\theta & 0 & 0 \\ 0 & 0 & Z_N \cos^2\theta & -Z_N \sin\theta\cos\theta & 0 & 0 \\ 0 & -Z_T \sin\theta\cos\theta & -Z_N \sin\theta\cos\theta & Z_N \sin^2\theta + Z_T \cos^2\theta & 0 & 0 \\ 0 & 0 & 0 & 0 & Z_T \cos^2\theta & -Z_T \sin\theta\cos\theta \\ 0 & 0 & 0 & 0 & -Z_T \sin\theta\cos\theta & Z_T \sin^2\theta \end{bmatrix} \tag{16}$$

where θ is the angle between the crack and the horizontal direction, and Z_N and Z_T are the normal and tangential flexibility, which can be written as:

$$Z_N = \frac{8B_4}{3\sqrt{C_{11}C_{33}}} \frac{e}{1 - C_{13}^2 / \left(C_{11}C_{33}\right)} \tag{17}$$

$$Z_T = \frac{16}{3C_{44}} \frac{e}{\sqrt{\frac{C_{66}}{C_{44}} + B_4 - \frac{2C_{44}B_4}{\sqrt{C_{11}C_{33}} + C_{13} + 2C_{44}}}} \tag{18}$$

where B_4 can be expressed as:

$$B_4 = \sqrt{\frac{\left(\sqrt{C_{11}C_{33}} - C_{13}\right)\left(\sqrt{C_{11}C_{33}} + C_{13} + 2C_{44}\right)}{C_{33}C_{44}}} \tag{19}$$

So far, an anisotropic petrophysical model applicable to shale containing high-angle tectonic seams has been established, and the established model is utilized to simulate the actual working area.

3.2 Evaluation of gas content in shale gas reservoirs

3.2.1 Adsorption gas evaluation model. For shales at different depths, the adsorbed gas content calculated from well logs must be corrected for TOC and temperature to obtain isothermal adsorption parameters [26]. In this paper, based on the linear relationship between Langmuir volume and total organic carbon content, the temperature and total organic carbon content of isothermal adsorption line are corrected, so that isothermal adsorption parameters can be obtained for shales with different depths and properties. Temperature correction method:

$$V_{Lt} = 10^{-c_1 \times (T + c_2)} \tag{20}$$

$$P_{Lt} = 10^{c_3 \times (T + c_4)} \tag{21}$$

$$C_2 = \log V_L + \left(C_1 \times T_i\right) \tag{22}$$

$$C_4 = \log P_L + \left(-C_3 \times T_i\right) \tag{23}$$

The TOC correction method can be expressed as follows:

$$V_{Lc} = V_{Lt} \times \frac{TOC_{\lg}}{TOC_{iso}} \tag{24}$$

$$G_a = \frac{V_{Lc} \times p}{\left(p + p_{Lt}\right)} \tag{25}$$

3.2.2 Free gas evaluation models. In this thesis, the free gas content in shale in Anyang area of Hunan Province is calculated and analyzed by volumetric method, which is expressed as follows:

$$G_f = PV / T = P_0 V_0 / T_0 \tag{26}$$

Where P is the pressure corresponding to a certain shale burial depth, V is the pore volume, T is the formation temperature, and P_0, V_0, and T_0 are the pressure, free gas volume, and temperature under the special temperature and pressure conditions of 0°C and 101.325 kPa, respectively. In addition, V in Eq. can be obtained by calculation. Namely:

$$V = 0.01\varnothing / \rho \tag{27}$$

After obtaining the adsorbed and free gas of the shale, the total gas content of the shale is obtained expressed as:

$$G_t = G_a + G_f \tag{28}$$

4. Analysis of Physical Parameters of Shale Gas Reservoirs in Hunan Province

According to the study, the Silurian penstock shale in the middle and peripheral margins of the Cambrian Xiaoyanxi Formation under the jurisdiction of Hunan Province is widely distributed, rich in organic matter, with a moderate degree of thermal evolution, and has the prospect of industrialized development. Shale gas has been found in the western part of Hunan and Hubei province. Still, the thickness of its high-quality reservoirs is small, the lateral distribution is unstable, and the gas content varies greatly, so it is difficult to explore and deploy shale gas. There is an urgent need to reveal the physical properties of its shale gas reservoirs and gas content to theoretically guide shale gas development and exploration.

4.1 Calculation of Physical Parameters of Shale Gas Reservoirs

4.1.1 Total organic carbon content. Total organic carbon (TOC) content is an indicator of shale organic matter abundance, which is the most important control factor for shale gas accumulation. The uranium (U) content of the logged natural gamma energy spectrum correlates with the formation's organic carbon content. Taking the shale section of 2462.7~2579.3m in 5# of Hunan Anhua Cambrian Xiaoyanxi Formation as the research object, the multiple linear regression model of TOC given in the previous section was used to make a rendezvous plot of uranium content and measured TOC content of logging wells, and its specific distribution is shown in Fig. 2.

The results show that the correlation between the uranium content and this shale section's logged measured TOC content is good, and the model fit R2 is 0.851. 5# of Hunan Anhua Cambrian Xiaoyanxi Formation can be used to establish a model for calculating the TOC content of Xiaoyanxi Formation shale with the logged U content data. The average TOC content of the 2462.7~2579.3m shale section of Hunan Anhua Cambrian Xiaoyanxi Formation 5# is 1.79% using the logging model. The average TOC content of the logged wells is 1.75%, and the absolute error of the two is only 2.23%. The TOC results obtained by the multiple regression model match the TOC data of the logged wells. The TOC content of section 5# of the Xiaoyanxi Formation calculated by the multiple regression method better agrees with the tested TOC content, and the established calculation model is more applicable.

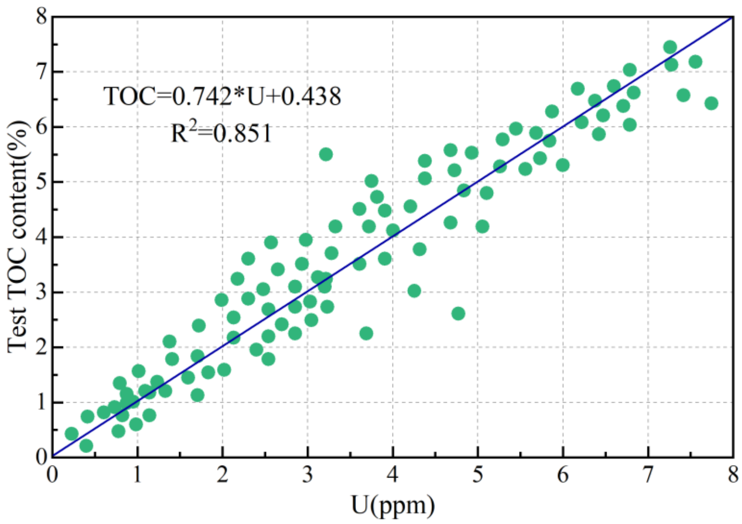

Fig. 2. Multivariate linear regression fitting result

4.1.2 Calculation of mineral composition. In shale gas reservoirs, after accurately finding the mud content, a multi-mineral component volumetric model of complex lithology was used to calculate the content of feldspathic (quartz, feldspar), calcareous (calcite), and dolomitic (dolomite, ferro-dolomite) classes. The established volume model features four mineral compositions: hard gypsum, quartz, calcite, and dolomite, i.e., the standard four-mineral selection method is used. Combined with the mineral composition calculation method given in the previous section, the method was applied to the formation mineral component calculation in the 5# shale gas exploration well of the Xiaoyanxi Formation in the study area, and the calculation results were compared with the core analysis data. The comparison of the model calculation results is shown in Figure 3.

The average errors of calcite, dolomite, feldspar, and mud content calculations for the Little Smokey Creek Formation 5# shale formation are 9.45%, 9.32%, and 7.49%, respectively. The feldspar content calculations have a large deviation, mainly in the Little Smokey Creek Formation 5# X-diffraction analyses of feldspar, which have a high content and slightly large deviation from the calculated results. The average error is 10.79% after excluding the 5#X data of the Little Smokey Creek Formation. The mud content is more accurate, and the calcite and dolomite content are calculated with some errors. Compared with the XRD diffraction analysis data, the accuracy of the calculation results of the complex lithology volume model is high overall, which can meet the requirements of the basic production application of shale gas exploration in Hunan Province.

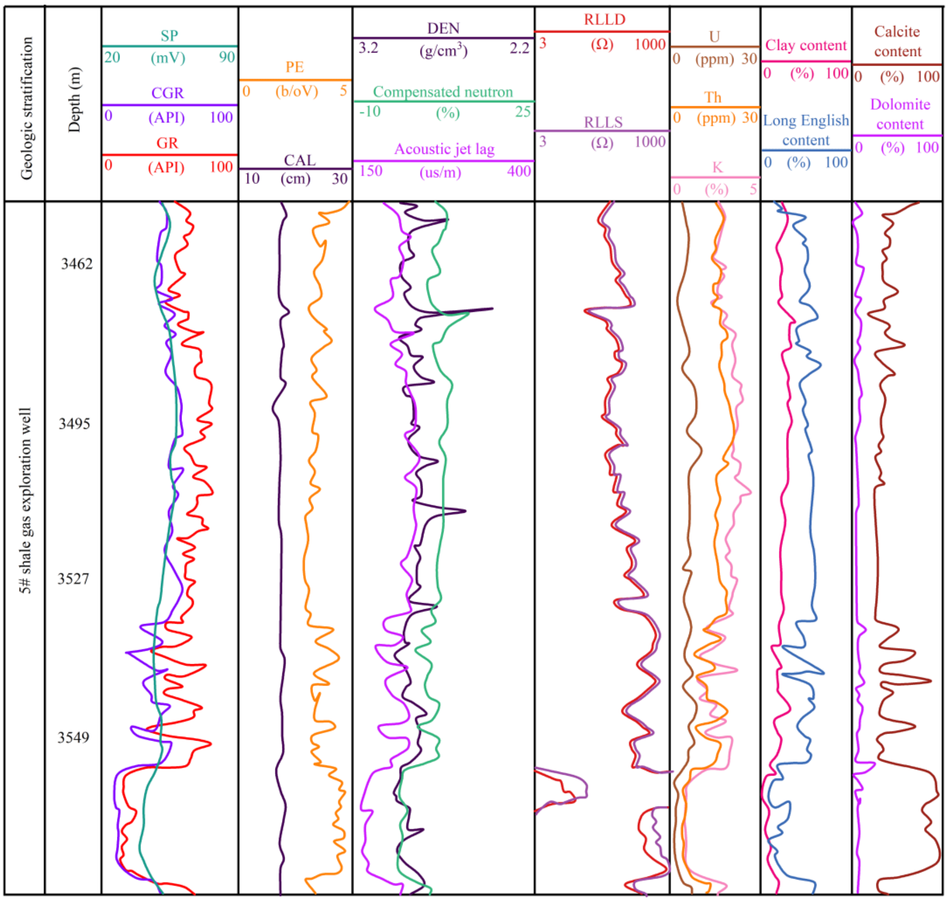

Fig. 3. Mineral composition calculation results

4.1.3 Pore structure characterization. A thin organic-rich layer is common in shale with a thin grain structure. The organic-rich layer consists of many organic-rich bands and clay minerals on both sides under a scanning electron microscope. The organic-rich bands are dominated by micaceous fragments, indicating that the organic matter in the layer is more derived from the parent material of terrestrial higher plants, followed by filaments and part of the solid asphalt. Based on the sample data of Xiaoyanxi Formation 5# in Anhua, Hunan Province, the occupancy of different pore structures within the organic-rich shale layer of Xiaoyanxi Formation 5# is obtained by using large-area image splicing and void recognition techniques, as shown in Figure 4.

As can be seen from the figure, the percentage of pores within the organic matter-rich grain layer is, from largest to smallest, clay mineral intergranular pores (50.18%) > organic matter pores (31.95%) > dissolution pores (13.01%) > residual compaction pores (4.86%). Although the organic matter in the organic-rich grain layer is often concentrated in the smooth layer, and the organic matter pores are developed in large quantities, the clay mineral intergranular pores in the grain layer are still the main pore type due to the control of the overall organic matter content is still low. The organic matter pores in the organic matter-rich grain layer are mainly distributed in the ranges of 100-250 nm and 450-600 nm, which correspond to the intervals of organic matter pores and clay mineral inter-crystalline pores with a large amount of development. The pore peaks of organic matter pore development are also formed by two types of organic matter pore with different development degrees. The peaks smaller than 100 nm are mainly contributed by dispersed asphaltene organic matter, and such small and dense organic matter pores will provide a large amount of storage space for adsorbed gas. With the increase of thermal evolution, a portion of the original small organic matter pores within the asphaltene are enlarged due to hydrocarbon generation. New large organic matter pores are formed by contacting, connecting, and merging between the pores. This type of pore space provides the pore size peak at 400~450 nm. It can be hypothesized that with the change of maturity, the peaks of the major developing pore diameters of the organic matter pores will also change. Based on the comparison of SEM images, it was found that the pores with this type of peaks are mainly composed of organic matter and clay minerals in the symbiotic complex; on the one hand, the clay minerals in the organic-clay complex have a catalytic effect on the pore generation of organic matter. On the other hand, it is also found that microporous seams are easily developed in the edge contact interface of the organic matter-clay composite. The microporous seams are consistent with the production of clay minerals. The pore space of the originally undeveloped organic matter is significantly increased after being transformed by the microporous seams.

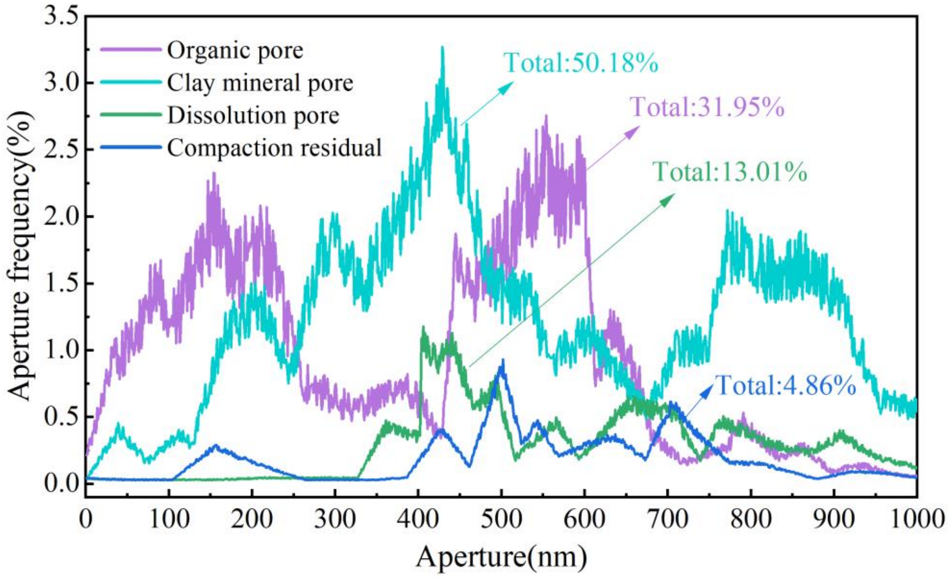

Fig. 4. The proportion of different pore structures

4.2 Petrophysical properties of shale gas reservoirs

4.2.1 Inelastic Response Orthotropic Analysis. Factors such as organic matter and fluid endowment make shale have inelastic characteristics. The dispersion and attenuation in shale are mainly caused by the viscous friction between the inorganic particles and the surface of casein, and the degree of organic matter enrichment and maturity together control the dispersion and attenuation characteristics of shale reservoirs. Based on the physical model of shale established in the previous paper and considering the inelastic characteristics of shale due to the factors of organic matter and fluid storage, an inelastic petrophysical model of shale gas reservoir is constructed to establish the coupling relationship between microscopic physical characteristics and inelastic parameters of shale. Figure 5 shows the variation curves of elastic parameters with frequency under different volume fractions of organic matter mixtures.

It can be observed that the volume fraction of the organic matter mixture has a greater effect on the elastic properties of shale. The longitudinal wave velocity, transverse wave velocity, longitudinal wave impedance, and longitudinal and transverse wave velocity ratios show a decreasing trend with the increasing volume fraction of organic matter mixture. When the volume fraction of the organic matter mixture increases from 0 to 0.25, the relative changes of longitudinal wave velocity, transverse wave velocity, and longitudinal wave impedance are about 22.47%, 20.58%, and 30.42%, which is mainly because the relatively softer materials, such as casein and fluid, reduce the elastic stiffness of the shale. In contrast, the relative change in the longitudinal and transverse wave velocity ratio is smaller, only 0.87%, when the volume fraction of the organic matter mixture is increased from 0 to 0.25. Thus, the elastic properties of shale petrophysics are affected by the volume fraction of organic matter mixtures, and such effects need to be considered when analyzing the physical properties of shale gas reservoirs.

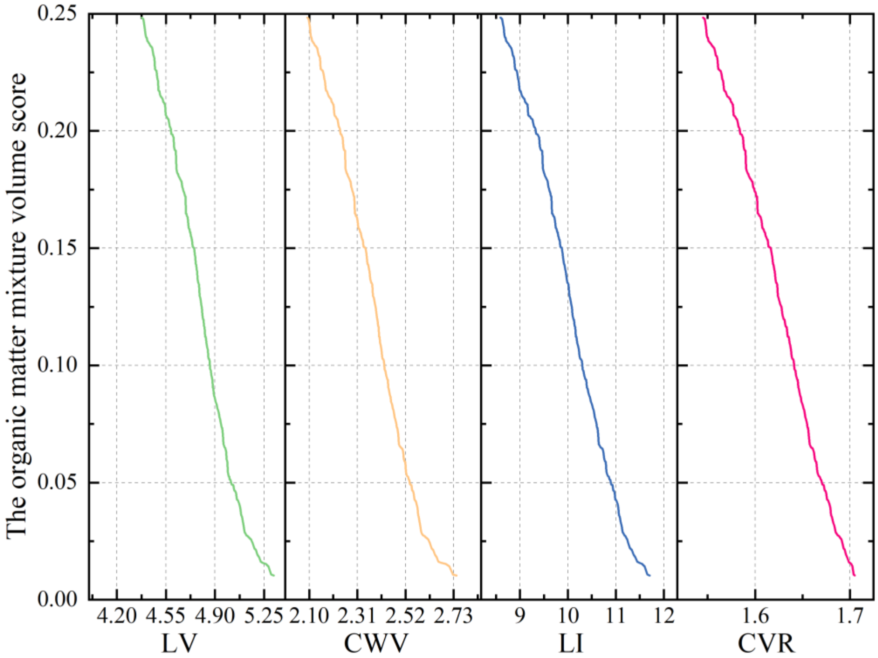

Fig. 5. Elastic parameters change the curve of frequency

4.2.2 Shale petrophysical template analysis. The organic matter content reflects the hydrocarbon generation capacity of shale to a certain extent. It controls shale gas production, while the mud content can indicate the formation's brittleness characteristics to a certain extent and determines the fracturing modification effect. Based on the petrophysical model and the analysis of the factors influencing the elasticity parameters, the petrophysical templates of TOC content and mud content were constructed with Poisson's ratio and longitudinal wave impedance as the horizontal and vertical coordinates, and the petrophysical templates were calibrated by combining with the logging data. Figure 6 shows the constructed petrophysical templates of longitudinal wave impedance and Poisson's ratio, whereas Figures 6(a) and (b) show the petrophysical templates of TOC content and mud content, respectively.

As can be seen from the figures, both longitudinal wave impedance decreases with increasing TOC content. It increases with decreasing mud content, while the relationship between Poisson's ratio and TOC content is more complicated. When the mud content is higher than 25%, TOC content increases, and Poisson's ratio decreases, and when the mud content is lower than 25%, TOC content increases, and Poisson's ratio increases. Comparison of the distribution characteristics of the recorded well data and the templates revealed that the distribution characteristics of TOC content and mud content of the scatter data are basically consistent with the overall trend of the template changes, and a small amount of the scatter data coincide poorly with the mineral fractions and contents, average porosity, and average water saturation selected for the establishment of the templates. Therefore, the TOC content and mud content can be reasonably analyzed based on this shale petrophysical template.

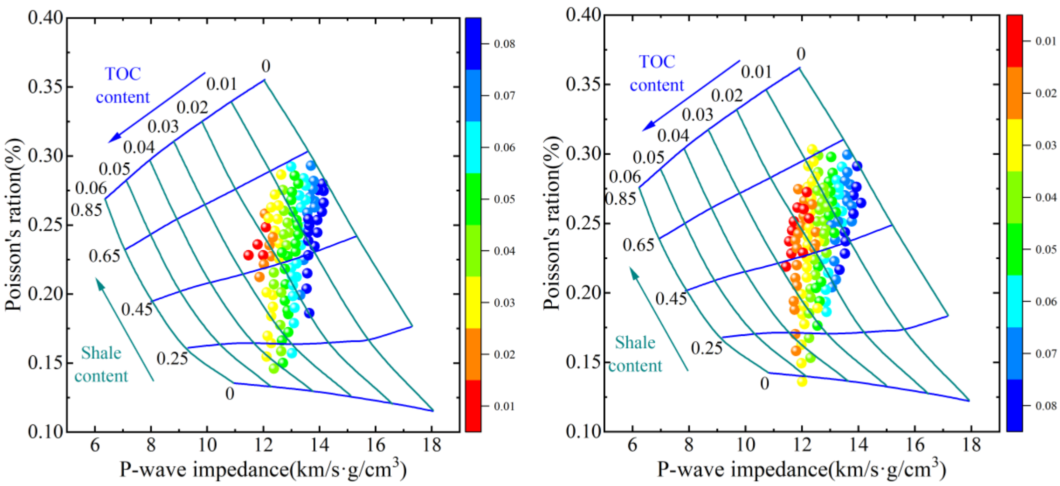

(a) TOC content (b) Clay content

Fig. 6. Longitudinal impedance and poison scale

4.3 Calculation of gas content in shale gas reservoirs

4.3.1 Gas content of shale gas reservoirs. There are direct and indirect methods to evaluate the gas content of shale; the direct method is the on-site desorption experiment, and the indirect method has various kinds. The most commonly used method is the measurement of adsorbed gas content. Based on the calculation methods of adsorbed gas and free gas given in the previous section, 10 samples from 5# of Xiaoyanxi Formation in Anhua, Hunan Province, were subjected to an isothermal adsorption test, and the corresponding data were obtained for the calculation of shale gas content. The results of the total shale gas content calculation are shown in Figure 7.

The methane gas content varies from 0.87 to 8.41 cm^3/g, among which the methane adsorption capacity of mud shale is mostly in the range of 2.19-4.06 cm^3/g, 40% of the mud shale samples have methane gas content lower than 2.19 cm^3/g, and the methane adsorption capacity of the two coal samples of shale is 4.06 and 8.41 cm^3/g, respectively, which is significantly higher than the methane adsorption capacity of mud shale. This is comparable to the average adsorption capacity of 1.75-2.84 cm^3/g of shale in the South China North Basin, Lower Yangzi region, and Sichuan Basin studied by previous researchers, which is lower than that of marine shale. Because of the good gas content of shale layers, joint exploration and deployment are recommended to investigate shale gas resource potential in Anhua, Hunan Province, where coal bed shale gas is an important component of coal system natural gas. The on-site desorption test can directly obtain the shale gas content, including lost, desorbed, and residual gas. The study shows that the desorbed gas content of shale in 5# of Xiaoyanxi Formation is 0.95cm^3/g and 1.09cm^3/g, and the total gas content is 2.43cm^3/g and 2.21cm^3/g. The total gas content of shale is larger than the lower limit value of shale gas industrial development of 0.5cm^3/g. Therefore, shale gas in Xiaoyanxi Formation of Anhua, Hunan Province, has a good potential for exploration.

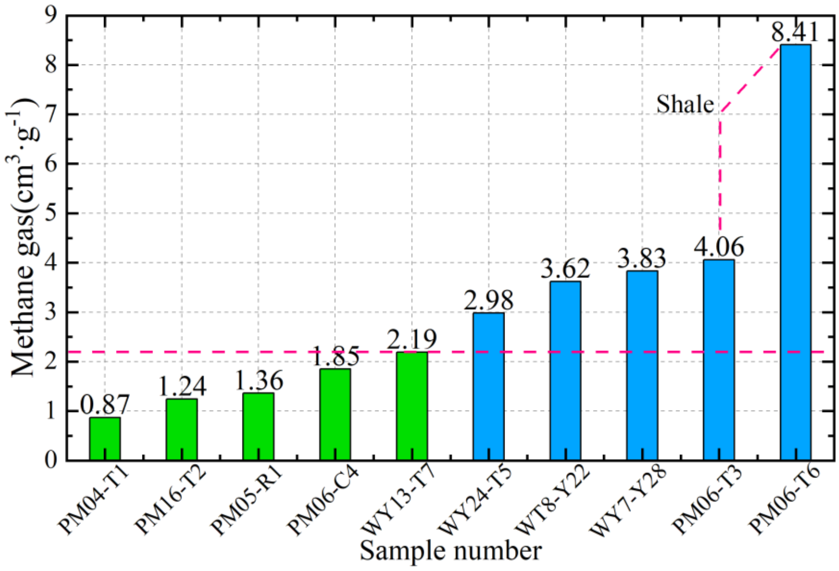

Fig. 7. Shale gas total gas quantity calculation results

4.3.2 Gas correlation of shale reservoirs. The gas content in shale 5# of Xiaoyanxi Formation in Anhua, Hunan Province, shows that the gas measurement value is very low, but the analysis of the isothermal adsorption test shows that the experiments show that the adsorption gas content is larger under the temperature of 25°C and the pressure of 15 MPa. The correlation results of shale adsorption gas content with pressure and TOC are shown in Fig. 8.

The figure shows that the adsorption amount of shale has a linear relationship with pressure and TOC, showing that shale has a strong adsorption capacity. The measured gas content in shale 5# of Hunan Anhua Xiaoyanxi Formation is 1.09 cm^3/g, which reaches the potential of shale gas development. The organic carbon content in the core of 5# shale of Hunan Anhua Xiaoyanxi Formation is slightly higher than that of 4#, but the development density of cracks in the reservoir is much higher than that of 4#, which is the fundamental reason for the enrichment of shale gas. The next exploration direction is the fracture development area in the Hunan Anhua Xiaoyanxi Formation. According to the comprehensive analysis of regional geology, the area of Hunan Anhua Xiaoyanxi Formation located near the Baoding-Cili fracture zone is characterized by the development of tiny fractures sandwiched between several faults, extremely developed coordinated fractures, and a burial depth of 1,950m, which may be a shale gas-rich area, and the exploration efforts should be increased.

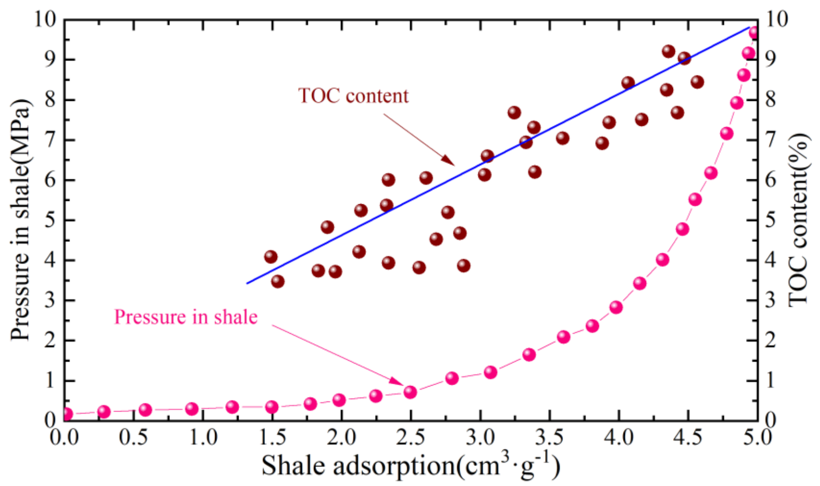

Fig. 8. The correlation results of shale adsorption

5. Conclusion

In this paper, based on the shale logging data of 5# of Xiaoyanxi Formation in Anhua, Hunan Province, the data analysis of shale gas reservoir physical properties in Hunan Province is carried out by using petrophysical modeling, reservoir physical parameters, and gas content evaluation. The average TOC content calculated by the shale short using the logging model is 1.79%, which is only 2.23% higher than the absolute error of the actual data. The pore structure in the shale reservoir is expressed from largest to smallest as clay mineral intergranular pores (50.18%) > organic matter pores (31.95%) > dissolution pores (13.01%) > residual compaction pores (4.86%). When the volume fraction of the organic matter mixture was increased from 0 to 0.25, the relative changes in longitudinal wave velocity, transverse wave velocity, and longitudinal wave impedance were about 22.47%, 20.58%, and 30.42%. In comparison, the relative change of longitudinal and transverse wave velocity ratio was only 0.87%. Overall, the gas content of shale in 5# of Anhua Xiaoyanxi Formation in Hunan Province ranges from 0.87 to 8.41 cm^3/g, significantly higher than the lower limit value for industrial development of shale gas. We can increase the exploration efforts along the Anhua Xiaoyanxi Formation to obtain more shale gas to alleviate the energy predicament.

Funding

Fund name: Technical support for verification of strategic mineral target area in eastern China (Changsha Center) (Funding Number: DD20242960).

References

[1] Basso, G. L., Rosa, F., Garcia, D. A., & Cumo, F. (2018). Hybrid systems adoption for lowering historic buildings PFEC (primary fossil energy consumption)-A comparative energy analysis. Renewable energy, 117, 414-433.

[2] Alvarez, G. E., Marcovecchio, M. G., & Aguirre, P. A. (2020). Optimization of the integration among traditional fossil fuels, clean energies, renewable sources, and energy storages: An MILP model for the coupled electric power, hydraulic, and natural gas systems. Computers & Industrial Engineering, 139, 106141.

[3] Arutyunov, V. S., & Lisichkin, G. V. (2017). Energy resources of the 21st century: problems and forecasts. Can renewable energy sources replace fossil fuels. Russian Chemical Reviews, 86(8), 777.

[4] York, R., & Bell, S. E. (2019). Energy transitions or additions?: Why a transition from fossil fuels requires more than the growth of renewable energy. Energy Research & Social Science, 51, 40-43.

[5] Lin, B., & Xu, B. (2020). How does fossil energy abundance affect China's economic growth and CO2 emissions?. Science of the Total Environment, 719, 137503.

[6] Novotnik, B., Nandy, A., Venkatesan, S. V., Radović, J. R., Fuente, J. D. L., Nejadi, S., ... & Larter, S. R. (2020). Can fossil fuel energy be recovered and used without any CO 2 emissions to the atmosphere?. Reviews in Environmental Science and Bio/Technology, 19, 217-240.

[7] Caporin, M., & Fontini, F. (2017). The long-run oil–natural gas price relationship and the shale gas revolution. Energy Economics, 64, 511-519.

[8] Zhang, B., Shan, B., Zhao, Y., & Zhang, L. (2020). Review of formation and gas characteristics in shale gas reservoirs. Energies, 13(20), 5427.

[9] Wang, Q., & Li, R. (2017). Research status of shale gas: A review. Renewable and Sustainable Energy Reviews, 74, 715-720.

[10] Pan, X. P., Zhang, G. Z., & Chen, J. J. (2020). The construction of shale rock physics model and brittleness prediction for high-porosity shale gas-bearing reservoir. Petroleum Science, 17, 658-670.

[11] Wenzhi, Z., Ailin, J., Yunsheng, W., Junlei, W., & Hanqing, Z. (2020). Progress in shale gas exploration in China and prospects for future development. China Petroleum Exploration, 25(1), 31.

[12] Taghavinejad, A., Sharifi, M., Heidaryan, E., Liu, K., & Ostadhassan, M. (2020). Flow modeling in shale gas reservoirs: A comprehensive review. Journal of Natural Gas Science and Engineering, 83, 103535.

[13] Zhang, J., Shi, M., Wang, D., Tong, Z., Hou, X., Niu, J., ... & Huang, Y. (2022). Fields and directions for shale gas exploration in China. Natural Gas Industry B, 9(1), 20-32.

[14] Sun, H., Yao, J., Cao, Y. C., Fan, D. Y., & Zhang, L. (2017). Characterization of gas transport behaviors in shale gas and tight gas reservoirs by digital rock analysis. International Journal of Heat and Mass Transfer, 104, 227-239.

[15] Middleton, R. S., Gupta, R., Hyman, J. D., & Viswanathan, H. S. (2017). The shale gas revolution: Barriers, sustainability, and emerging opportunities. Applied energy, 199, 88-95.

[16] Akilu, S., Padmanabhan, E., & Sun, Z. (2021). A review of transport mechanisms and models for unconventional tight shale gas reservoir systems. International Journal of Heat and Mass Transfer, 175, 121125.

[17] Zou, C., Zhao, Q., Dong, D., Yang, Z., Qiu, Z., Liang, F., ... & Hu, Z. (2017). Geological characteristics, main challenges and future prospect of shale gas. Journal of Natural Gas Geoscience, 2(5-6), 273-288.

[18] Lyu, Q., Tan, J., Li, L., Ju, Y., Busch, A., Wood, D. A., ... & Hu, R. (2021). The role of supercritical carbon dioxide for recovery of shale gas and sequestration in gas shale reservoirs. Energy & Environmental Science, 14(8), 4203-4227.

[19] Striolo, A., & Cole, D. R. (2017). Understanding shale gas: Recent progress and remaining challenges. Energy & Fuels, 31(10), 10300-10310.

[20] Chen, S., Gong, Z., Li, X., Wang, H., Wang, Y., & Zhang, Y. (2021). Pore structure and heterogeneity of shale gas reservoirs and its effect on gas storage capacity in the Qiongzhusi Formation. Geoscience Frontiers, 12(6), 101244.

[21] Wang, S. (2018). Shale gas exploitation: Status, problems and prospect. Natural Gas Industry B, 5(1), 60-74.

[22] Shengxiu Wang,Ye Zhang,Wei Wang,Yang Yang,Qiaoli Wang,Chuan Yu... & Yao Xu. (2024). Insights into the Co-Exploration Potential of Gas in the Shale and Tight Sandstone of the Lower Silurian Formation in the Gongtan Syncline Area in Southeastern Sichuan Basin, SW China. Energies(15),3735-3735.

[23] Akinniyi A. Akinwumiju,Dorothy Satterfield & Jordan J.J. Phethean. (2024). Evaluation of shale oil and gas plays - Part I: Shale reservoir property modelling of the North Sea Kimmeridge Clay Formation. Marine and Petroleum Geology106824-.

[24] Xinhui Deng,Xinze Kang,Duo Yang,Wei Fu & Teng Luo. (2024). Advancing Quantitative Seismic Characterization of Physical and Anisotropic Properties in Shale Gas Reservoirs with an FCNN Framework Based on Dynamic Adaptive Rock Physics Modeling. Applied Sciences(4).

[25] Shi Kai Jian,Li Yun Fu,Wensheng Duan,Gengxin Peng,Suo Cheng,Yongliang Tang & Duoming Zheng. (2024). Rock-physics modeling and pre-stack seismic inversion for the Cambrian superdeep dolomite reservoirs in Tarim Basin, Northwest China. Marine and Petroleum Geology106973-106973.

[26] Yang Liu,Chenggang Xian & Xiaoqing Huang. (2024). Characteristics of Micro–Nano-Pores in Shallow Shale Gas Reservoirs and Their Controlling Factors on Gas Content. Energies(7).